

## Fabrication of Polyaniline Nanoparticles Using Microemulsion Polymerization

Jyongsik Jang\*, Jungseok Ha, and Sunhee Kim

*Hyperstructured Organic Materials Research Center, School of Chemical and Biological Engineering,  
Seoul National University, Seoul 151-742, Korea*

*Received September 29, 2006; Revised October 16, 2006*

**Abstract:** Polyaniline (PANI) nanospheres, 4 nm in diameter, were fabricated by the microemulsion polymerization of octyltrimethyl ammonium bromide (OTAB). The size of the PANI nanoparticles could be controlled as functions of the surfactant concentration, surfactant spacer length and polymerization temperature. The diameter of the PANI nanospheres decreased with increasing surfactant concentration and decreasing temperature. The PANI nanoparticles revealed enhanced conductivity compared to conventional bulk PANIs. In addition, the PANI nanoparticles could be applied as optically transparent conducting materials due to their high conductivity and the nanosize effect. With 9 wt% PANI in the PC matrix, the PANI/PC film exhibited a conductivity of  $8.9 \times 10^{-3}$  S/cm and transparency exceeding 95% over the entire visible light range.

**Keywords:** conducting polymers, nanoparticles, microemulsion polymerization, polyaniline.

### Introduction

Conducting polymers are considered as an important class of materials because of their potential applications in various electronic devices such as chemical sensors, electrochromic displays and light emitting diodes.<sup>1</sup> Among the various conducting polymers, polyaniline (PANI) is one of the most promising conducting materials due to its facile synthesis, low cost, remarkable environmental stability, relative high conductivity, and unique redox behavior.

On the basis of these superiorities, PANI has been applied in the fields of antistatic material, anticorrosion coating, battery and energy storage, organic light-emitting diode (OLED), and chemical sensor.<sup>2-6</sup> To date, PANI nano-materials have been mainly synthesized by the precipitation, dispersion, emulsion polymerization, and electrospinning method.<sup>7-19</sup> Lee *et al.* reported the fabrication of conducting polymer nanofiber using PANI/PEO blend by electrospinning technique. The diameter of PANI nanofiber was about 100 nm and the conductivity of nanofiber exhibited up to 33 S/cm at 50 wt% of PANI content.<sup>20</sup>

Recently, several researchers have synthesized polymer nanoparticles using microemulsion polymerization.<sup>21-25</sup> This approach utilizes the nanometer-sized micelles as "nanoreactor", which were formed from self-assembly of surfactant molecules in solvent. Therefore, the morphology of resultant polymer nanoparticles is largely dependent on the micelle structure derived from the surfactant assembly such as

spherical, cylindrical, and layer structures. In previous work, we reported that microemulsion polymerization was the facile route to produce conducting polymer nanostructures ranged from 10 to 50 nm.<sup>22,26,27</sup> However, it is difficult to control the size of PANI nanoparticles and synthesize monodisperse and highly conductive PANI nanoparticles due to particle-particle aggregation and complicated polymerization process under acidic environmental condition. Therefore, it is desirable to develop a simple and reliable method to manufacture PANI nanoparticles with the well-defined and uniform spherical structure for optically transparent conducting application.

Herein, we report the fabrication of monodisperse and nanometer-sized PANI spheres as small as 4 nm using microemulsion polymerization. The size of PANI nanoparticle was controlled as functions of different surfactants, surfactant concentrations and polymerization temperatures. In addition, we also investigated the conductivity of PANI nanoparticles depending on the polymerization temperature and surfactants. On the basis of nanosize and high conductivity, PANI nanoparticles could be applied as optically transparent conducting materials.

### Experimental

**Materials.** Octyltrimethylammonium bromide (OTAB) and dodecyltrimethylammonium bromide (DeTAB) were purchased from Tokyo Kasei Koggo (TKI, Tokyo, Japan) and used without further purification. Monomer, aniline and redox initiator, ammonium persulfate (APS) were purchased

\*Corresponding Author. E-mail: jsjang@plaza.snu.ac.kr

from Aldrich (Milwaukee, WI, USA) and used as received. Polycarbonate (PC) was also purchased from Aldrich.

**Preparation of PANI Nanoparticles.** A variable amount of cationic surfactant was magnetically stirred in 40 mL of distilled water at 3 °C. In a typical fabrication of PANI nanoparticles, 1 g (10.7 mmol) of aniline monomers were added dropwise to the surfactant solution and 1.23 g (5.3 mmol) of APS and 22 g (33 mmol) of 1.5 M HCl were added to the mixed solution. The chemical oxidation polymerization proceeded with magnetically stirring for 3 hr. After polymerization, the reaction product was placed in the separate funnel. An excess ethanol and distilled water were poured into the funnel alternately to remove surfactants and to precipitate PANI nanoparticles. The PANI nanoparticles were retrieved and dried in a vacuum oven at room temperature. Polymerization temperature and surfactant concentration were varied to investigate the size and conductivity of PANI nanoparticles.

**Preparation of PANI Nanoparticles/PC Composites.** PANI nanoparticles and PC (Mw 30,600) were blended in chloroform to make transparent conducting composites. A variety ratio of PANI/PC composites were fabricated from 1 wt% filler content to 9 wt% filler content. The mixed solution was stirred and spin-coated onto a glass slide using a spinner. The thickness of fabricated films was estimated with an Alpha Step surface profiler and could be controlled by varying the spinning speed. All films were approximately 280 nm thick, which could be maintained well. Transparency of the films was measured with UV/Vis spectrometer and the conductivity of composites was also determined by the standard four probe method.

**Instrumental Analysis.** The electrical conductivity was determined by the four probe method using a Keithley 2400. Bright-field transmission electron microscope (TEM) images were taken with a JEOL 2000EX II microscope operated at an accelerating voltage of 200 kV. The UV-VIS spectra were taken with a Perkin-Elmer Lambda-20 spectrometer. The Fourier-transform infrared (FTIR) spectra were recorded on a Bomem MB 100 spectroscope in the absorption mode at a resolution of 4 cm<sup>-1</sup> and 32 scans. Energy-dispersive X-ray (EDX) analysis was performed using a Philips CM 20 microscope. Spin coating was conducted with a PWM32 spinner (Headway Research, Inc.). Film thickness was estimated with Alpha-step 500 surface profiler. Wide angle X-ray diffraction analysis was estimated with 3000 PTS X-Ray Diffractometer (Rich. Seifert & Co.). Raman spectrum was analyzed with LabRam HR (Jobin-Yvon).

## Results and Discussion

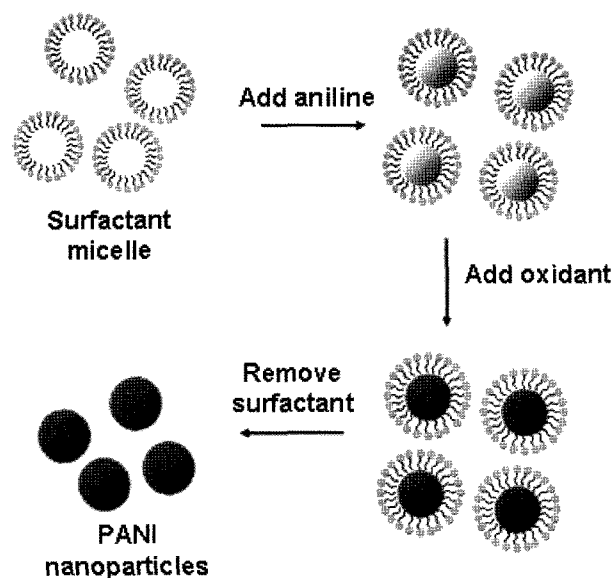
PANI nanoparticles were fabricated with respect to different surfactant concentration, surfactant spacer length, and polymerization temperature by microemulsion polymerization. Cationic surfactants such as OTAB and DeTAB were used

to form micelles as nanoreactors. OTAB and DeTAB, surfactants with short chains, were chosen to make PANI spheres as small as possible. Hexyltrimethylammonium bromide (HTAB) was not considered to be proper surfactant. HTAB could not form highly ordered structures because of the weak hydrophobic interactions associated with the short C-6 moiety.<sup>25</sup> Surfactants with hydrocarbon chain longer than C-16 were not adequate for the low temperature microemulsion due to high viscosity and liquid crystalline behavior.

The fabrication of PANI nanoparticles was illustrated in Scheme I. The formed micelles from OTAB were used as nanoreactors. Aniline monomers were added dropwise to the micelles, and chemical oxidation polymerization was proceeded by APS. The synthesized PANI powders had typical green color of emeraldine salt form.

FTIR spectroscopic analysis supported the observation that the prepared polymer nanospheres consisted of PANI. Figure 1 shows the FTIR spectrum of PANI nanoparticles prepared using 0.4 M OTAB at 3 °C. In the FTIR spectrum, the peak at 823 cm<sup>-1</sup> is attributed to out-of-plane bending vibration of C-H on para-disubstituted rings and the bands at 1128 and 1572 cm<sup>-1</sup> are designated to the stretching vibration of C=C quinonoid ring. In addition, the characteristic peak at 1487 cm<sup>-1</sup> is due to the stretching vibration of C=C benzenoid ring at 1487 cm<sup>-1</sup> and the band at 1299 cm<sup>-1</sup> is ascribed to the stretching vibration of C-N.

Raman spectrum of the PANI nanoparticle synthesized using 0.4 M OTAB at 3 °C is shown in Figure 2. The band at 1135 cm<sup>-1</sup> results from C-H bending of quinoid or benzenoid ring. The peak at 1318 and 1381 cm<sup>-1</sup> are due to C-N stretching and electron absorption of free charge carrier, respectively. N-H bending is observed at 1459 cm<sup>-1</sup>. The



**Scheme I.** Schematic illustration for the surfactant templating of PANI nanoparticles.

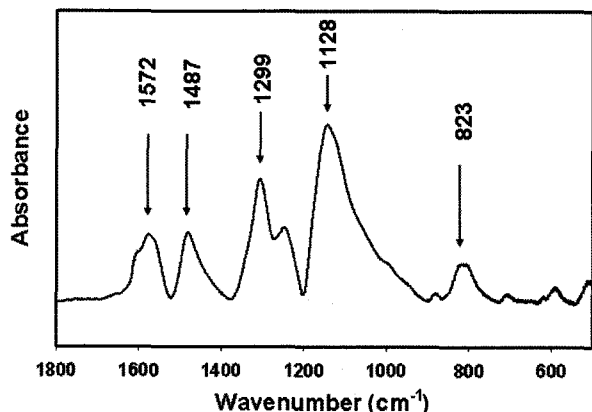


**Figure 1.** FTIR spectrum of polyaniline nanoparticles prepared using 0.4 M OTAB at 3 °C.

absorption at 1586 cm<sup>-1</sup> was attributed to the C-C stretching of benzenoid ring.

In Figure 3, UV-vis spectrum of PANI nanoparticles dis-

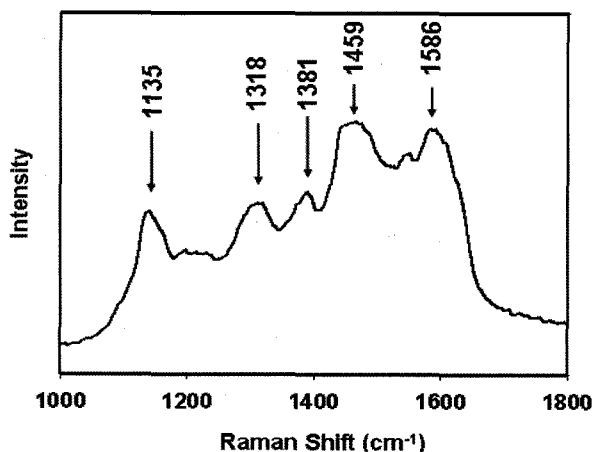


**Figure 2.** Raman spectrum of polyaniline nanoparticles synthesized using 0.4 M OTAB at 3 °C.

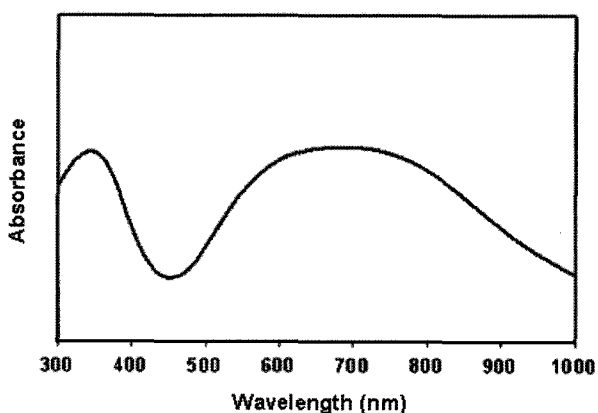
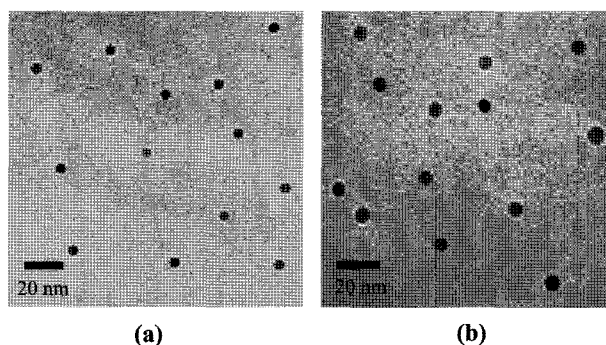


**Figure 3.** UV-vis spectrum of polyaniline nanoparticles synthesized using 0.4 M OTAB at 3 °C.

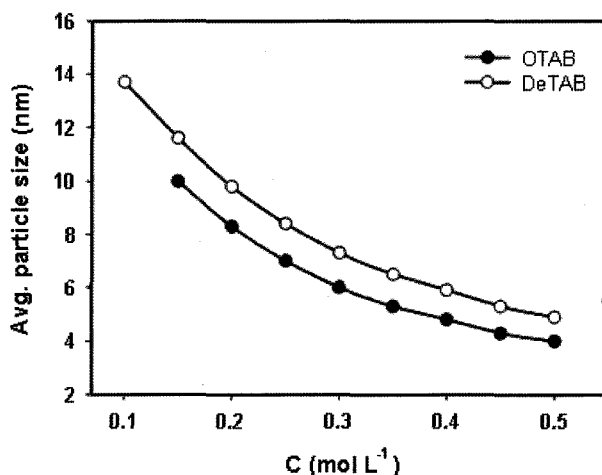
persed in ethanol is manifested. There are two critical peaks of PANI emeraldine salt nanospheres: the peak at 340 nm is due to  $\pi$ - $\pi^*$  transition and the peak at 660 nm corresponds to the exciton transition. The exciton transition is caused by the electron transition from benzene ring to a quinoid ring along the PANI chain. In addition, the <sup>1</sup>H NMR analysis of the PANI nanoparticles showed no methyl resonance which might come from residual surfactants. From the spectroscopic analyses, it could be concluded that the surfactants were completely removed and PANI nanoparticles were successfully synthesized.

Figure 4(a) represents TEM image of the PANI nanoparticles polymerized using 0.5 M OTAB at 3 °C. The TEM image revealed that PANI nanoparticles with an average diameter of as *ca.* 4 nm were spherical and monodisperse. In the case of 0.5 M DeTAB, the TEM image of PANI nanoparticles represented the spherical shape with *ca.* 6 nm in diameter (Figure 4(b)).

Figure 5 illustrates the variation of PANI nanoparticle sizes as functions of the surfactant spacer length and surfac-



**Figure 4.** TEM micrographs of PANI nanoparticles prepared at 3 °C using (a) OTAB and (b) DeTAB.



**Figure 5.** Average change in particle size as a function of surfactant concentration. The average nanoparticle size was determined by TEM (50 particles counted).

tant concentration. At the same concentration of surfactant, the diameter of PANI nanoparticles using OTAB was smaller than that of DeTAB. This might result from smaller size of surfactant micelle with shorter chain length due to the reduced critical packing parameter (CCP).<sup>28</sup> In addition, total number of micelles in solution at the same concentration increases with decreasing the alkyl chain length.<sup>29</sup> Therefore, the smaller amount of monomer existent in a micelle of OTAB leads to the reduction in the nanoparticle size. The size of PANI nanoparticle also decreased with increasing the surfactant concentration. The increment in surfactant concentration produces the larger number of micelles, resulting in the particle size reduction. Judging from these results, the diameter of PANI nanoparticle can be readily controlled by the spacer length of surfactant and surfactant concentration.

The conductivity of these products was measured by the standard four probe method. For the conductivity measurement, pellets of approximately 1 cm diameter and 0.15 millimeter in thickness were prepared by pressing the powdered sample. Table I represents the conductivity and average diameter of PANI nanoparticles as a function of polymerization temperature. As the polymerization temperature increased, the nanoparticle diameter also increased due to the increased mobility of surfactant chains.<sup>22</sup> The conductivity of PANI nanoparticles using 0.5 M OTAB at 3 °C was as high as 84.6 S/cm. It has been reported that the conductivity of HCl-doped PANI ranged from 0.1-10 S/cm.<sup>30</sup> Importantly, the conductivity of PANI nanoparticle showed nearly one order of magnitude higher than that of PANI previously reported by conventional polymerization. As the polymerization temperature decreased, the conductivity of PANI nanoparticle increased drastically. The lower conductivity at higher polymerization temperature seems to be caused by the enhanced reaction of oxygen with the aniline molecules and the formation of structural defects such as carbonyl groups on aniline ring.<sup>31-33</sup> Energy dispersive X-ray analysis (EDAX) was used to characterize the constituent elements of

PANI nanoparticles. The atomic percent of oxygen increased gradually with increasing polymerization temperature; 7.2% (3 °C), 11.6% (25 °C), and 17.7% (60 °C). These results indicate that the decrement in conductivity at higher temperature results from a large number of structural defects on the PANI chain molecules. The conductivity change of PANI nanoparticle can be also explained according to the PANI particle size. The diameter of PANI nanoparticles increased as the polymerization temperature increased. For 4 nm PANI nanosphere, polymerization occurred at the limited dimension of nanoreactor and resultant polymer had the highly compact and order-inducing structures.<sup>34</sup> At 60 °C, the average diameter of PANI nanosphere increased up to *ca.* 32 nm and the polymer chains became more randomly oriented. This disordered structure and chain defects tend to decrease the conductivity of PANI nanoparticle at the elevated temperature. In the case of DeTAB, the longer spacer of surfactant provides more free volume inside the micelle and, forms larger PANI nanoparticle. Therefore, it could be explained that PANI nanospheres using DeTAB showed the lower conductivity compared with OTAB.

These results could be also supported by X-ray diffraction (XRD) analysis presented in Figure 6. The XRD patterns of PANI nanoparticles synthesized at different polymerization temperature exhibited sharp peaks at  $2\theta = 20^\circ$  and  $26^\circ$  indicating the presence of high crystallinity and condensed structure. The peak centered at  $2\theta = 20^\circ$  is ascribed to periodicity parallel to the polymer chain and the latter peak may be caused by the periodicity to the polymer chain.<sup>24</sup> This crystalline structure could be explained by the fact that the PANI nanospheres were prepared in nanosize micelles, thus proceeded in denser and more compact structures. In addition, the peaks at  $2\theta = 20^\circ$  and  $26^\circ$  became sharper and stronger as the polymerization temperature decreased. These ten-

**Table I. The Conductivity and Average Diameter of PANI Nanospheres Obtained at Different Polymerization Temperatures**

Surfactant	Temperature (°C)	Avg. Diameter (nm)	Conductivity (S/cm)
OTAB (0.5 M)	3	4.1	84.6
	25	18.0	28.4
	60	32.2	2.9
DeTAB (0.5 M)	3	6.2	76.4
	25	21.4	22.9
	60	37.1	1.7

OTAB: Octyltrimethylammonium bromide.

DeTAB: Dodecyltrimethylammonium bromide.

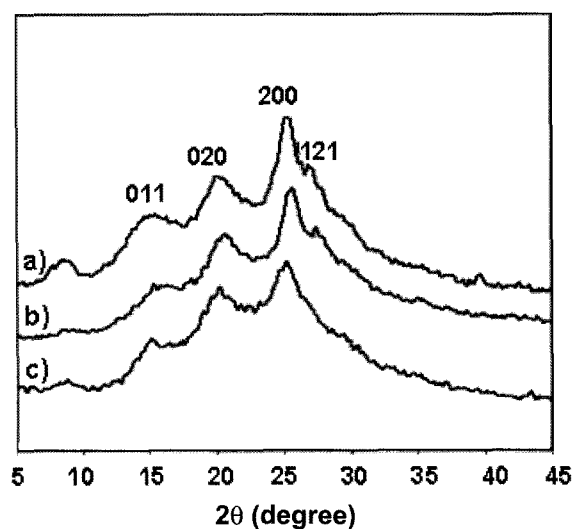


**Figure 6.** XRD patterns of PANI nanoparticles prepared at (a) 3 °C, (b) 25 °C, and (c) 60 °C using OTAB.

**Table II.** The Ratio of Half-Width to Height of X-Ray Diffraction Peak Prepared in the Condition of Different Temperatures

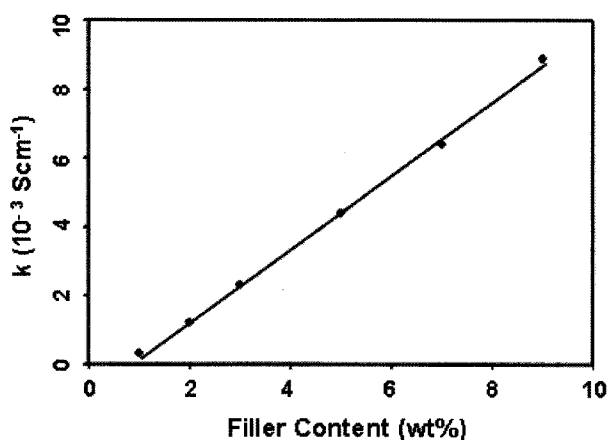
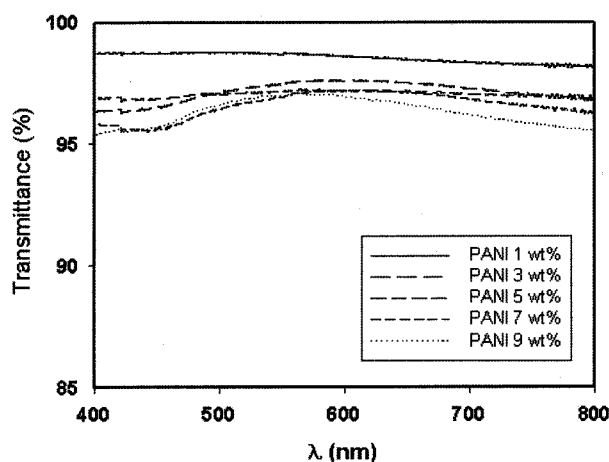
Temperature (°C)	The Ratio of (HW/H)	
	020 Peak	200 Peak
3	0.041	0.016
25	0.049	0.022
60	0.052	0.031

HW/H : Half-width to height.

encies have been proved by the ratio of half-width to height (HW/H) of X-ray diffraction peak, which reflects the order of the polymer backbone (the smaller the value of HW/H, the higher the crystallinity). As shown in Table II, the ratio of (HW/H) decreased with decreasing polymerization temperature. Especially below 25 °C, a new peak was found at 28° suggesting the more developed crystallinity at the lower temperature. These results are in good agreement with the relationship between the crystallinity of conducting polymer and its electrical conductivity: the greater the degree of crystallinity, the higher the conductivity.<sup>35</sup>

It is anticipated that these PANI nanoparticles can be applied as optically transparent conducting materials due to their high conductivity and ultrafine nanosize. In general, PC is a typical transparent amorphous polymer and has been used for compact disks and glass substitutes. The PANI nanoparticles were blended with PC in chloroform. PANI nanoparticle, which has typically conductivity of 84.6 S/cm and average particle diameter of 4 nm, was selected for this experiment. Figure 7 represents the conductivity of PANI/PC nanocomposite as a function of PANI nanofiller content.

From the viewpoint of filler content, the conductivity of PANI/PC nanocomposite increased in proportion to PANI content in PC matrix. The conductivity of  $0.7 \times 10^{-3}$  S/cm

**Figure 7.** Conductivity of PC/PANI nanocomposite as a function of PANI nanofiller content.**Figure 8.** Transparency of PC/PANI nanocomposite as a function of PANI nanofiller content.

was obtained with 1 wt% of PANI nanoparticle and increased up to  $8.9 \times 10^{-3}$  S/cm at 9 wt% of PANI content. It can be explained that the formation of local electronic paths is favorable with increasing the filler content which is ultrafine and uniform PANI nanosphere. The transparency of these films is shown in Figure 8. To be transparent polymer composite film, the average diameter of conductive fillers should be smaller (approximately  $0.2 \mu\text{m}$ ) than half of the shortest wavelength of visible light. The transparency of these films decreased with increasing the amount of PANI nanoparticles. However, the transparency even at 9 wt% filler content was higher than 95% over the entire visible light range. PANI nanofillers were well dispersed in PC matrix, resulting in transparent polymer composites. Therefore, PANI nanoparticles could be used as effective nanofillers for optically transparent conducting polymer materials.

## Conclusions

PANI nanoparticles with diameter of *ca.* 4 nm were successfully fabricated by microemulsion polymerization. The size of PANI nanoparticle could be systematically tuned as functions of surfactant spacer length, surfactant concentration and polymerization temperature. The diameter of the PANI nanosphere decreased with increasing surfactant concentration and decreasing temperature. The PANI nanoparticle revealed the enhanced conductivity compared to the conventional bulk PANIs. The conductivity of PANI nanoparticle increased up to 84.6 S/cm at 3 °C compared with 2.9 S/cm at 60 °C. Importantly, PANI/PC nanocomposite film showed the conductivity of  $8.9 \times 10^{-3}$  S/cm and the transparency of above 95% over the entire visible light range even at 9 wt% of PANI content in PC matrix. Therefore, PANI nanospheres might be expected to be applied as conducting nanofillers of optically transparent conducting material.

**Acknowledgements.** This work was supported by the Brain-Korea 21 Program of the Korea Ministry of Education and by Hyperstructured Organic Materials Research Center (HOMRC) in Seoul National University.

## References

- (1) J. Jang, *Adv. Polym. Sci.*, **199**, 189 (2006).
- (2) J. Keum, C. S. Ha, and Y. Kim, *Macromol. Res.*, **14**, 401 (2006).
- (3) Q. Pei, G. Yu, C. Zhang, Y. Yang, and A. J. Heeger, *Science*, **269**, 1086 (1995).
- (4) U. Asawapirom, F. Bulut, T. Farrell, C. Gadermaier, S. Gamerith, R. Guntner, T. Kietzke, S. Patil, T. Piok, R. Montenegro, B. Stiller, B. Tiersch, K. Landfester, E. J. W. List, D. Neher, C. S. Torres, and U. Scherf, *Macromol. Symp.*, **212**, 83 (2004).
- (5) D. Chaudhuri, A. Kumar, I. Rudra, and D. D. Sarma, *Adv. Mater.*, **13**, 1548 (2001).
- (6) X. Zhang, W. J. Goux, and S. K. Manohar, *J. Am. Chem. Soc.*, **126**, 4502 (2004).
- (7) J. Y. Kwon, E. Y. Kim, and H. D. Kim, *Macromol. Res.*, **12**, 303 (2004).
- (8) P. Manisankar, C. Vedhi, and G. Selvanathan, *J. Polym. Sci. A*, **43**, 1702 (2005).
- (9) H. Qiu and M. Wan, *J. Polym. Sci. A*, **39**, 3485 (2001).
- (10) H. Xia and Q. Wang, *J. Appl. Polym. Sci.*, **87**, 1811 (2003).
- (11) D. Chattopadhyay, M. Chakraborty, and B. M. Mandal, *Polym. Int.*, **50**, 538 (2001).
- (12) M. Wan and J. Li, *J. Polym. Sci. A*, **37**, 4605 (1999).
- (13) J. Stejskal, P. Kratochvil, and M. Helmstedt, *Langmuir*, **12**, 3389 (1996).
- (14) P. S. Rao, S. Subrahmanya, and D. N. Sathyanarayana, *Synth. Met.*, **9201**, 1 (2002).
- (15) J. Huang, S. Virji, B. H. Weiller, and R. B. Kaner, *J. Am. Chem. Soc.*, **125**, 314 (2003).
- (16) Z. Zhang, Z. Wei, and M. Wan, *Macromolecules*, **35**, 5937 (2002).
- (17) G. M. Do Nascimento, P. Corio, R. W. Novickis, M. L. A. Temperini, and M. S. Dresselhaus, *J. Polym. Sci. A*, **43**, 815 (2005).
- (18) M. V. Kulkarni, A. K. Viswanath, R. Marimuthu, and T. Seth, *J. Polym. Sci. A*, **42**, 2043 (2004).
- (19) M. Wan and J. Li, *J. Polym. Sci. A*, **38**, 2359 (2000).
- (20) S. H. Lee, J. W. Yoon, and M. H. Suh, *Macromol. Res.*, **10**, 282 (2002).
- (21) J. Li, K. Fang, H. Qiu, S. Li, W. Mao, and Q. Wu, *Synth. Met.*, **145**, 191 (2004).
- (22) J. Jang, J. H. Oh, and G. D. Stucky, *Angew. Chem. Int. Ed.*, **41**, 4016 (2002).
- (23) J. Jang and K. Lee, *Chem. Commun.*, 1098 (2002).
- (24) F. Yan and G. Xue, *J. Mater. Chem.*, **9**, 3035 (1999).
- (25) X. J. Xu, L. M. Gan, K. S. Siow, and M. K. Wong, *J. Appl. Polym. Sci.*, **91**, 1360 (2004).
- (26) J. Jang and J. H. Oh, *Adv. Mater.*, **16**, 1650 (2004).
- (27) J. Jang and J. H. Oh, *Adv. Funct. Mater.*, **15**, 494 (2005).
- (28) S. Zhou, F. Yeh, C. Burger, and B. Chu, *J. Phys. Chem. B*, **103**, 2107 (1999).
- (29) H. J. Reiss, *Colloid Interface Sci.*, **53**, 61 (1975).
- (30) J. Stejskal, A. Riede, D. Hlavata, J. Prokes, M. Helmstedt, and P. Holler, *Synth. Met.*, **96**, 55 (1998).
- (31) G. Boara and M. Sparpaglione, *Synth. Met.*, **72**, 135 (1995).
- (32) N. Kuramoto and A. Tomita, *Polymer*, **38**, 3055 (1997).
- (33) J. Lei, Z. Cai, and C. R. Martin, *Synth. Met.*, **46**, 53 (1992).
- (34) J. Duchet, R. Legras, and S. Demoustier-Champagne, *Synth. Met.*, **98**, 113 (1998).
- (35) W. Luzny and E. Banka, *Macromolecules*, **33**, 425 (2000).